Energy Based Earthquake Load and Resistance Design

A. Surahman
Faculty of Civil and Environmental Engineering, Institut Teknologi Bandung

SUMMARY:
During earthquake, structural components absorb energy induced by the ground shaking. Hence earthquake loads can be expressed in energy terms. Selected records of earthquakes from various parts of the world are analyzed to identify governing parameters. Energy evaluations show that energy is a consistent parameter and structural performance is determined not only by the peak ground acceleration and spectral acceleration, but also by the earthquake input energy. Various structural members and components are evaluated. The resistance of a structural component is based on its energy carrying capacity during an earthquake and is measured in terms of the cumulative ductility before it reaches a structural failure. The design is based on cumulative ductility demand and capacity of structural components. It is shown that the energy based seismic design as a new design philosophy and method provides a consistent concept to deal with earthquake phenomenon.

Keywords: energy input, equivalent velocity, unit velocity, cumulative ductility, energy coefficient

1. INTRODUCTION

The current design practice uses design forces based on design response spectral acceleration S_a, defined by Eqn. (1.1) for a fundamental period of the structure T less than T_0 [ASCE 2010]

$$S_a = S_{DS}\left(0.4 + 0.6\frac{T}{T_0}\right) \tag{1.1}$$

by Eqn. (1.2) for T between T_0 and T_S

$$S_a = S_{DS} \tag{1.2}$$

and Eqn. (1.3) for T between T_S and T_L

$$S_a = \frac{S_{D1}}{T} \tag{1.3}$$

where S_{DS} is the design earthquake response acceleration parameter at short period, S_{D1} is the design earthquake response acceleration parameter at T = 1 second, T_S is the ratio of S_{D1} over S_{DS}, and T_0 is one fifth of T_S. In many other countries, to maintain conservative design, Eqn. (1.3) is also used for T larger than T_L and hence the formula for this period range and T_L are not discussed here. The base shear V is then defined in Eqn. (1.4)

$$V = C_S W \tag{1.4}$$

where W is the total building weight and C_S is the seismic coefficient defined as $I(S_a/R)$ where S_a is defined by Eqn. (1.2) for short period (T less than T_S) or Eqn. (1.3) for longer period where I is the importance factor, taken as 1 for ordinary buildings, and R is the response modification factor. The force distribution along the building height is defined as

$$F_i = \frac{W_i h_i^{\,k}}{\sum_{j=1}^{n} W_j h_j^{\,k}} V \tag{1.5}$$

where F_i is the lateral force acting on the level i, W_i is the weight of the floor at level i, h_i is the floor elevation from the ground at level i, k is the exponential factor, and n is the number of stories.

In recent years many energy based seismic design formulations have been proposed [Akiyama 1985 and 1988, Cosenza and Manfredi 1996, Fajfar 1996, Kalkan and Kunath 2007 and 2008, Surahman 2007 and 2011, Surahman et al 2008, Surahman and Merati 1992, and Teran-Gilmore and Jirsa 2004]. The approach uses an energy equation given in Eqn. (1.6) developed by [Akiyama 1985 and 1988].

$$\int_0^{t_d} M\ddot{y}\dot{y}dt + \int_0^{t_d} C\dot{y}^2 dt + \int_0^{t_d} F(y)\dot{y}dt = \int_0^{t_d} F(t)\dot{y}dt \tag{1.6}$$

where t_d is the duration of the earthquake. The right hand term is the total input energy E_I which, to eliminate size effects, is then expressed by an equivalent velocity V_E defined in Eqn. (1.7)

$$V_E = \sqrt{\frac{2E_I}{M}} \tag{1.7}$$

where M is the total reactive mass of the building. Only part of the input energy will cause building damage. The rest are stored as elastic strain energy, kinetic energy, or dissipated by the damping. This portion of the energy is called the energy attributable to damage E_D. An empirical formula for the corresponding equivalent velocity, called the equivalent velocity attributable to damage V_D, is given by Eqn. (1.8) [Akiyama 1985]:

$$V_D = \frac{V_E}{1 + 3\xi + 1.2\sqrt{\xi}} \tag{1.8}$$

where ξ is the damping coefficient (percentage of critical damping). The energy attributable to damage is absorbed by members in the form of internal work given by Eqn. (1.9) [Akiyama 1985]

$$E_D = \alpha F_Y \delta_Y (0.5 + \eta) \tag{1.9}$$

where F_Y is the member yield strength, δ_Y is the member yield displacement, η is the cumulative ductility as a damage measure, hence also called cumulative damage, and α is the energy coefficient, reflecting the detailing characteristics [Surahman 2007]. This equation shows that more flexible or stronger members suffer less damage. The cumulative ductility η is defined by Eqn. (1.10)

$$\eta = \sum_{j=1}^{n} \mu_j \tag{1.10}$$

where μ_j is the plastic ductility ratio at the j-th yield excursion in the elastic-perfectly-plastic load-deformation relationships ($\mu = 0$ at yield point). Depending on the earthquake duration and the natural period of the structure, the ratio between the cumulative and maximum plastic ductility is normally between one to four [Akiyama 1985].

2. EARTHQUAKE PARAMETERS

To evaluate various earthquake parameters, selected earthquakes from various parts of the world (eastern and western sides of the Pacific Ocean, and Eurasian region from Turkey to India) have been evaluated as shown in Table 2.1. The parameters that have been calculated are the peak ground acceleration (PGA), the maximum dynamic magnification factor (DMF), and the maximum equivalent velocity V_E which are divided by PGA and T to give formulation generality into non-dimensional unit velocity U_E.

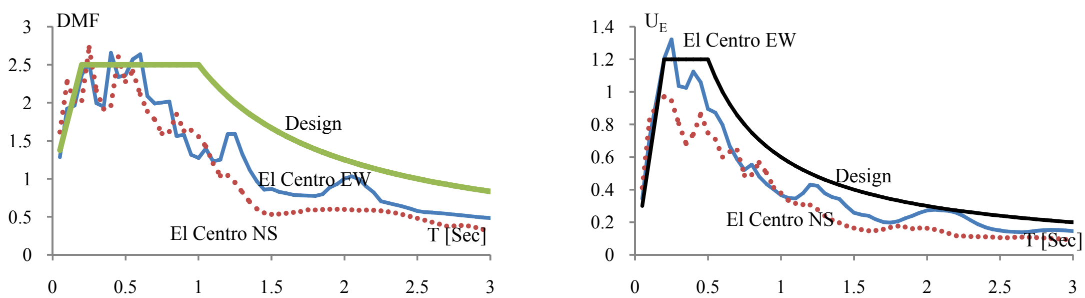

Figure 2.1: Dynamic Magnification Factor and Unit Acceleration

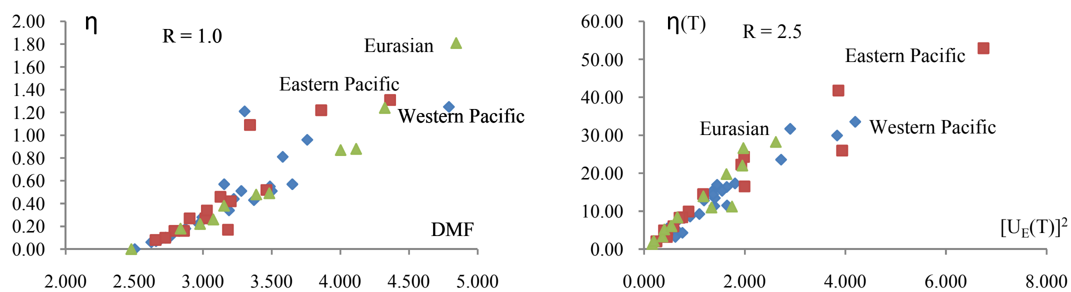

Figure 2.2: Cumulative Damage for R = 1 and R = 2.5 due to Various Earthquakes in the World

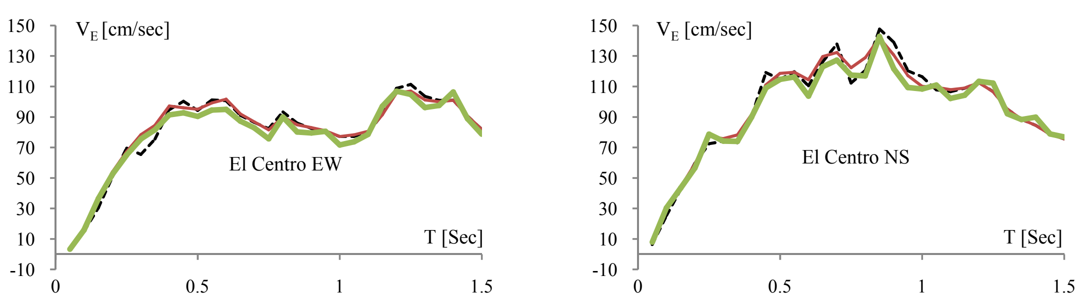

Figure 2.3. Equivalent Velocity for El Centro Earthquakes

The dynamic magnification factor DMF is basically equivalent to the spectral acceleration S_a. The response spectral acceleration defined by Eqn. (1.1) can be used for single degree of freedom structural models subjected to earthquake like El Centro, Northridge, and Parkfield earthquakes as shown in the left hand side of Fig. 2.1 and Table 2.1. For earthquakes with peak DMF far exceeding 2.5, the damage can be significant. For single degree of freedom structural models with R = 1, the relationship between DMF and the resulting maximum cumulative damages η, disregarding the natural period T in which it happens, are shown in the left side of Fig. 2.2 and the relationship is almost linearly correlated with a correlation coefficient of 0.912. For ductile structures with R larger than unity, the correlation between the DMF and η decreases as R becomes larger. In this case the use of energy approach is more appropriate. A normalized unit velocity U_E of 1.2 for T between 0.2 and 0.5 seconds, proportional to T for T < 0.2 and inversely proportional to T for T > 0.5 seconds can be used for the El Centro NS, San Fernando, and Taft earthquakes as shown on the right hand side of Fig. 2.1.

Table 2.1: Earthquake Peak Ground Accelerations, Dynamic Magnification Factors, and Unit Velocities

EQ Location, Year, Station, Direction	PGA	DMF	U_E	EQ Location, Year, Station, Direction	PGA	DMF	U_E
	[g]				[g]		
Nisqually, 2001, Tacoma, Dir 237	0.137	3.15	1.48	Kobe, 1995, Nishi Akashi, EW	0.509	4.36	1.16
Nisqually, 2001, Tacoma, Dir 327	0.155	3.19	1.25	Kobe, 1995, Nishi Akashi, NS	0.503	3.02	0.88
El Centro, 1940, El Centro, EW	0.215	2.66	1.32	Miyagi, 2011, Miyagi, EW	0.339	3.34	2.02
El Centro, 1940, El Centro, NS	0.313	2.73	0.97	Miyagi, 2011, Miyagi, NS	0.575	2.65	1.48
Taft, 1952, Lincoln School, 21	0.156	3.76	1.21	Chi-Chi, 1999, 23.6 N, 120.7 E, EW	0.968	3.18	0.78
Taft, 1952, Lincoln School, 111	0.178	3.22	1.05	Chi-Chi, 1999, 23.6 N, 120.7 E, NS	0.902	2.86	0.77
Loma Prieta, 1989, Corralitos, EW	0.644	3.37	0.88	Christchurch, 2011, Greendale, N55W	0.753	1.97	0.55
Loma Prieta, 1989, Corralitos, NS	0.479	2.87	0.88	Christchurch, 2011, Greendale, S35W	0.677	2.18	0.62
Northridge, 1994, Cedar Hill, EW	0.990	3.00	1.08	New Zealand, 1987, Matahina Dam, 83	0.256	3.20	1.01
Northridge, 1994, Cedar Hill, NS	1.779	2.50	0.82	New Zealand, 1987, Matahina Dam, 353	0.344	2.73	0.63
Parkfield, 1966, Cholame, 85	0.442	2.76	0.72	Jiashi, 1997, Jiashi, EW	0.300	3.03	0.92
Parkfield, 1966, Cholame, 355	0.367	3.50	0.84	Jiashi, 1997, Jiashi, NS	0.274	3.46	0.87
San Fernando, 1971, Lake Hughes, 21	0.366	3.58	1.05	Uttarkashi, 1991, Uttarkashi, 75	0.310	4.12	1.00
San Fernando, 1971, Lake Hughes, 291	0.283	4.79	1.27	Uttarkashi, 1991, Uttarkashi, 345	0.242	4.84	1.46
Mexico City, 1985, Michoacan, EW	0.156	2.97	1.30	Gazli, 1976, Karakyr, EW	0.608	2.84	1.48
Mexico City, 1985, Michoacan, NS	0.112	3.30	1.74	Gazli, 1976, Karakyr, NS	0.718	2.34	1.03
Mexico City, 1985, Zihuatanejo, EW	0.100	3.49	1.17	Tabas, 1978, Tabas, Longit	0.836	4.00	1.26
Mexico City, 1985, Zihuatanejo, NS	0.157	2.69	0.89	Tabas, 1978, Tabas, Transv	0.852	4.32	1.27
Off Shore Maule, 2010, San Pedro, EW	0.606	3.28	2.08	Spitak, 1988, Gukasian, EW	0.199	2.48	0.63
Off Shore Maule, 2010, San Pedro, NS	0.651	2.62	1.95	Spitak, 1988, Gukasian, NS	0.175	3.15	1.00
Valparaiso, 1985, Rapel, EW	0.089	3.65	1.44	Ducze, 1999, Bolu, EW	0.728	2.98	0.71
Valparaiso, 1985, Rapel, NS	0.223	2.04	0.71	Ducze, 1999, Bolu, NS	0.822	1.72	0.41
Hachinohe, 2011, Aomoriken, EW	0.337	2.79	2.10	Erzican, 1992, Erzican, EW	0.496	3.08	0.69
Hachinohe, 2011, Aomoriken, NS	0.186	3.86	2.62	Erzican, 1992, Erzican, NS	0.515	1.83	0.35
Kobe, 1995, Kakogawa, EW	0.251	3.13	1.26	Kocaeli, 1999, Ducze, EW	0.312	3.39	0.82
Kobe, 1995, Kakogawa, NS	0.345	2.90	1.24	Kocaeli, 1999, Ducze, NS	0.358	3.48	0.76

As shown by [Akiyama 1985 and 1988, Surahman 2007 and 2011, and Surahman and Merati 1992], the equivalent velocity expression is very consistent regardless of the structural configuration. Figure 2.3 shows the equivalent velocity for elastic single of degree model (R = 1), inelastic single degree of freedom model (R = 2.5) and four degree of freedom (four story) shear building models subjected to El Centro earthquakes. The equivalent velocity curves are basically identical so that the equivalent velocity (and consequently unit velocity) can be assumed to be unique for a same earthquake, site and direction. The η for single degree of freedom models with R = 2.5 at natural period T when U_E are at maximum (or conversely maximum η and the corresponding U_E) are calculated. Making use of Eqn. (1.9) for α =1, the resulting relationships using U_E^2 as variable, neglecting the DMF variable are shown in the right hand side of Fig. 2.2. The correlation is almost perfect, with the correlation coefficient of 0.953. This shows that the energy approach can accurately predict structural damage for inelastically designed structures.

3. STRUCTURAL COMPONENTS

The data for the energy or cumulative ductility capacity of several structural components have been experimentally determined as shown on Fig. 3.1 [Imran 2006, IRHS 2010, Mangkoesoebroto etl al 2003, Surahman and Moestopo 2000, and Surahman et al. 2003] and are summarized in Table 3.1. The larger energy coefficient (α value) indicates a larger energy absorption capacity, thus a better detailing. Graphically a large α value is indicated by a stocky hysteresis loop. This happens if strength reserve effects including strain hardening is dominant. On the other hand if strength degradation effects, including pinching, are dominant, the α value is smaller than unity. For elastic-perfectly plastic load deformation relationship the α value is equal to unity. When no sufficient data are available, the cumulative ductility capacity η_u can be predicted from the ultimate plastic ductility μ_u obtained from monotonic tests amongst others by using the Park and Ang model [Park et al 1985] which is reformulated in Eqn. (3.1) [Surahman 2007]:

$$\eta_u = \left(1 - \frac{\mu_{\max}+1}{\mu_u+1}\right)\frac{\mu_u}{\beta} + \frac{\mu_{\max}+1}{\mu_u+1}\mu_u \qquad (3.1)$$

where μ_{max} is the maximum plastic ductility that occurs during the cyclic loading, β is 0.15 for ductile structures and becomes larger for less ductile structures [Teran-Gilmore and Jirsa 2004 and Fajfar et al 1996].

Table 3.1. Energy Parameters for Various Components

Component	η	η/μ_u	α
Concrete Beam [Surahman and Moestopo 2000]	90.00 – 125. 00	8.40 – 11.67	0.50 – 0.60
Concrete Beam-1 [Mangkoesoebroto et al 2003]	102.23	14.6	0.8
Concrete Beam-2 [Mangkoesoebroto et al 2003]	146.12	20.7	0.9
Concrete Beam-1 [Imran et al 2006]	23.14	5.78	0.43
Concrete Beam-2 [Imran et al 2006]	9.69	3	0.35
Steel Beam [Surahman et al 2003]	41.92	9.32	1.46
Steel Connection-1 [Surahman and Moestopo 2000]	32.96	NA	0.33
Steel Connection-2 [Surahman and Moestopo 2000]	116.64	NA	0.69
Precast Element-1 [IRHS 2010]	3.64	NA	1.21
Precast Element-2 [IRHS 2010]	4.33	NA	1.63
Precast Element-3 [IRHS 2010]	2.33	NA	5.83
Precast Element-4 [IRHS 2010]	28.97	NA	0.44
Precast Element-5 [IRHS 2010]	27.27	NA	0.54
Precast Element-6 [IRHS 2010]	32.96	NA	0.33

For flexural members the F and δ terms in Eqn. (1.9) are replaced by M and θ. The cumulative damage due to plastic hinge rotation is derived using the same terminology used in the tests as shown in Fig. 3.1 and Table 3.1

$$\eta = \frac{3\Delta\theta(M_Y + M_O)}{L\phi_Y M_Y} \tag{3.2}$$

where L is the member length, $\Delta\theta$ is the plastic hinge rotation, M_Y is the yield moment, M_O is the moment at the opposite end (positive for double curvature), and ϕ_Y is the yield curvature.

Figure 3.1. Tests on Beam-Columns for Ductility Capacity

4. ENERGY BASED DESIGN

For design applications each two shear building (A and B) and frame (C and D) models, shown in Fig. 4.1 and Table 4.1 are evaluated. The earthquake load is measured in the terms of energy input, whereas the resistance in the terms of ductility capacity. The shear building responses are calculated using time history analysis whereas the frame responses are calculated by static pushover analysis.

Story	Mass	F_Y A Model	F_Y B Model
	[m]	[m PGA]	[m PGA]
4	2.5	4.0	2.5
3	3	7.7	5.5
2	3	10.2	8.5
1	3	11.5	11.5

Shear building with uniform stiffness, left

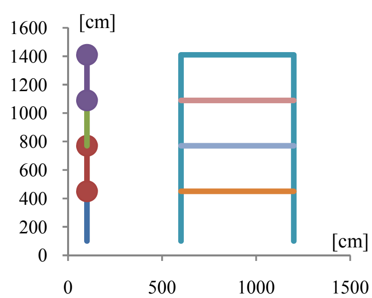

Mass	Section No C	D	C	D
[ton]	Column		Beam	
25	3	9	1	8
30	4	9	2	8
30	6	9	5	8
30	7	9	8	8

Frame loaded in accordance with Eqn. (1.5), right

Figure 4.1. Four Story Shear Building and Frame Models

The left hand side of Fig. 4.2 shows energy distribution among the story drawn cumulatively from bottom to the top in the A Model subjected to the El Centro EW earthquake. It can bee seen that with the F_Y design following Eqn. (1.9), the damages (η values) are concentrated in the lower stories of the structure. Figure 4.3 shows that despite having a larger DMF (thus larger S_a) the damages caused by the El Centro NS earthquake are significantly smaller. This is due to smaller unit velocity U_E in the NS direction as compared to the EW direction. Thus energy approach can predict ductility demand far more accurately than the presently used force based design method. Figure 4.4 shows that the Hachinohe NS earthquake with U_E twice as large causes far more damages then the El Centro earthquakes. This is due to the fact that the Hachinohe NS earthquake also has a larger dynamic magnification factor than the El Centro earthquakes. For many DMF values shown in Table 2.1 Eqns. (1.1) to (1.4) are sufficiently accurate to determine the base shear V.

Table 4.1. Section Numbers for Columns and Beams Used in the A and B Frame Models

Section No	Size	Weight	Area	Moment of Inertia	Section Modulus
	mm x mm	kg/m	cm^2	cm^4	cm^3
1	400x200	56.6	71.3	20008	1011
2	400x200	66	83.5	23694	1185
3	400x300	94.3	119.1	35604	1798
4	400x300	107	134.4	38653	1982
5	450x200	66.2	83.2	28680	1286
6	450x300	106	132.8	46762	2155
7	450x300	124	155.6	56037	2547
8	500x200	79.5	99.9	41843	1687
9	500x200	103	130.8	56490	2233

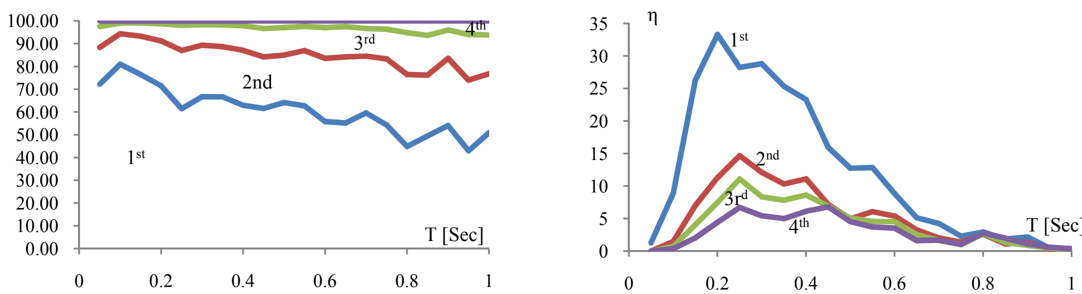

Figure 4.2. Energy Percentage distribution and η for A Model under El Centro EW Earthquake

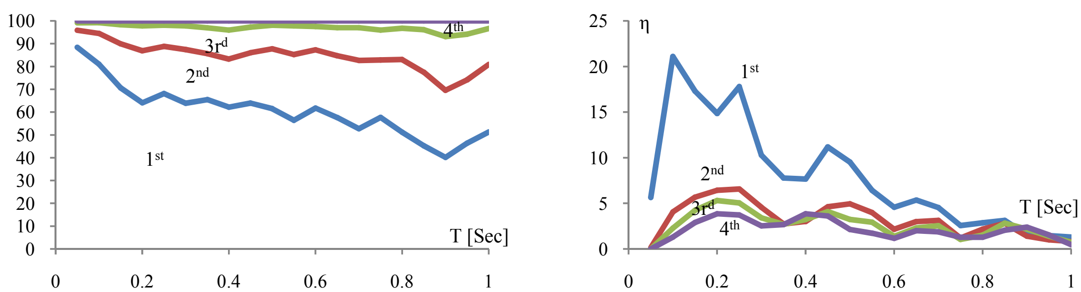

Figure 4.3. Energy Percentage Distribution and η for A Model under El Centro NS Earthquake

Figure 4.5 shows that when the design is slightly changed, that is the B model uses story strength proportional to the story weight, the damage distribution drastically changes, heavier in the upper stories. Weakening the upper story strength significantly reduces the damage in the first story. This is consistent with the constant energy principle that reduction of energy absorption in any part of the structure will be compensated by the increase of energy absorption in other part. Conversely increasing the upper story strength will increase the damage in the lower story. This cannot be detected in a force based design method. Models A and B are designed with the same R = 2.5 but different force distribution assumptions.

Figure 4.6 shows that for the A Model, the actual R values for lower stories are higher as also indicated by the η shown in Fig. 4.2. For the B model, the actual R values are higher in the upper stories as also indicated by η in Fig. 4.5. The deviation from 2.5 shows the deviation of the actual base shear from the one defined by Eqn. (1.4). The difference among R values of each story shows the deviation of force distribution from the one defined by Eqn. (1.5), showing that Eqn. (1.5) used for the A Model is a better estimate than assuming a constant proportion force distribution used for the B

Model. For an accurate estimate of force distribution the resulting curves shown on both sides of Fig. 4.6 merge into a single curve.

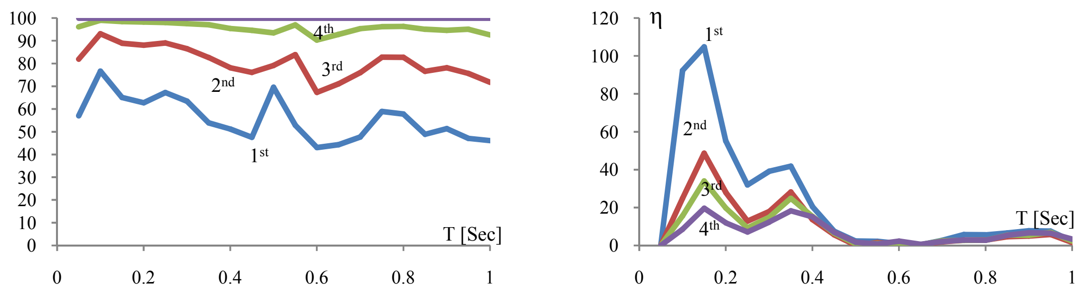

Figure 4.4. Energy Percentage Distribution and η for A Model under Hachinohe NS Earthquake

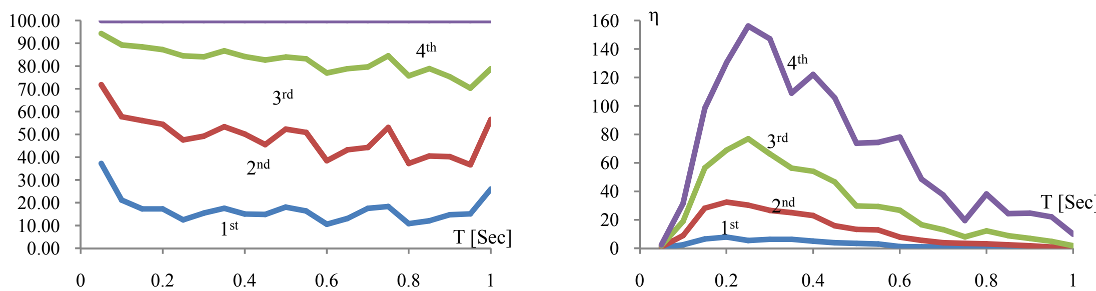

Figure 4.5. Energy Percentage Distribution and η for B Model under El Centro EW Earthquake

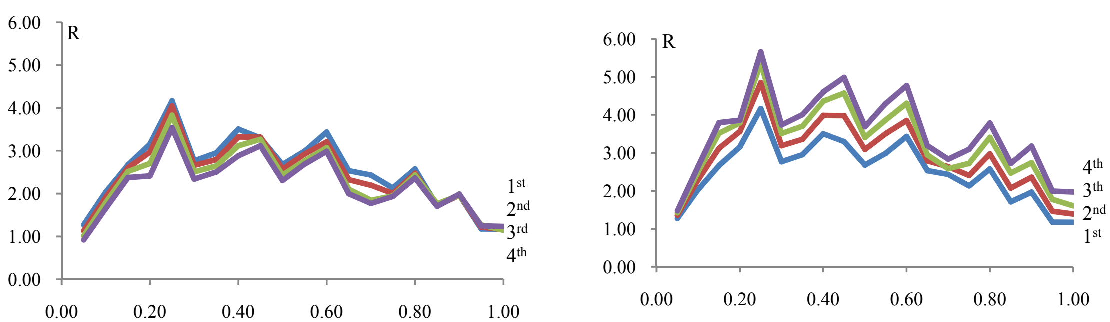

Figure 4.6. Actual R values for A and B Model under El Centro EW Earthquake

Figure 4.7 shows the relationships between the deformation and force acting on each story level of the C and D frame models during the pushover analysis. The C model gives an R value of 1.93 and overstrength factor Ω of 1.40 whereas the D model gives an R value of 2.50 and Ω value of 1.22. The first natural period of the frame are approximately 0.45 seconds. By using a PGA value of 0.25 g and the U_E of 1.2, the energy input on frames C and D models are calculated. For both frames, the external works done by the forces until the formation of the collapse mechanism at the fourth loading stage are below the energy input. Thus additional post collapse mechanism deformation as a fifth loading stage (without increasing the load) must be added to match the energy demand. The resulting deformation ductility ratios for the C model from first to fourth story at collapse stage are 5.65, 5.91, 3.97, and 3.69 respectively, and 5.91, 4.75, 4.31, and 3.92, at post-collapse stage. For the D models the values are 3.97, 3.53, 3.31, 3.12 and 6.46, 5.41, 5.03, 4.90 respectively. It can be seen that the post-collapse portion of energy input for D model is significantly larger than for the C model.

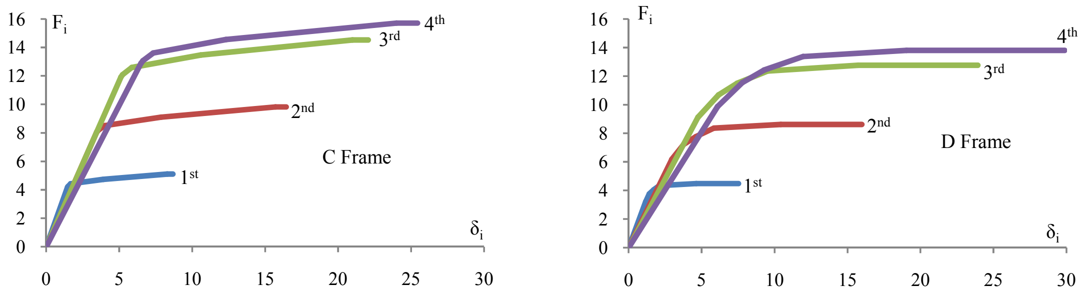

Figure 4.7. Load Deformation of C and D Frame Pushover analysis

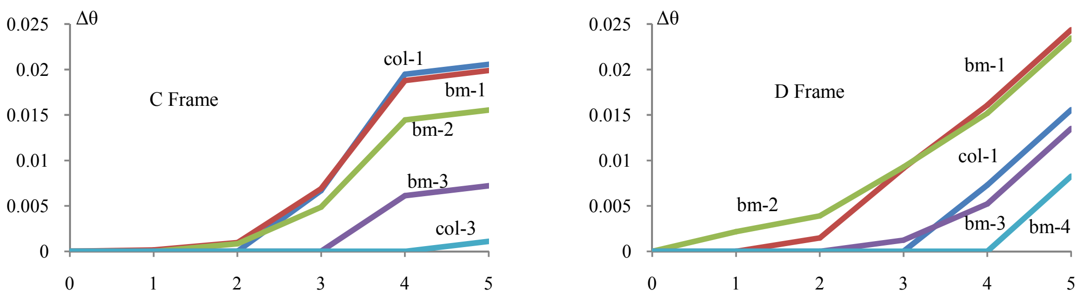

Figure 4.8. Plastic Hinge Rotation for Every Loading Stage Pushover Analysis

Figure 4.8 shows that for the C model the last hinge is formed in the column of the third story whereas for the D model in the beam of the fourth story, thus in accordance with the strong column weak beam concept. The cumulative damage and energy distribution among the members are shown in Table 4.2.

Table 4.2. Cumulative Damage and Energy Distribution Among Members

Frame C Model				Frame D Model			
Members	Cumulative Damage η		Energy Percentage	Members	Cumulative Damage η		Energy Percentage
	Collapse	Post			Collapse	Post	
Col-1	5.19	5.48	37.24	Col-1	1.26	2.69	26.37
Bm-1	3.73	3.95	28.34	Bm-1	3.19	4.84	32.40
Bm-2	2.87	3.08	22.15	Bm-2	2.71	4.19	23.77
Bm-3	1.21	1.43	10.29	Bm-3	0.84	2.16	11.67
Col-3	0.00	0.20	1.99	Bm-4	0.00	1.31	5.79

Despite the fact that the A, B, and D models are designed for R = 2.5, the resulting damage in the members of the frame models are significantly smaller than those of the shear building models. This is due to the differences in the analysis methods (pushover analysis versus time history analysis where the results depend on the earthquake acceleration used), number of members that can absorb energy (four yielding members in the shear building models as compared to five yielding members and two non yielding members in the frame models), and the percentage of strain energy. The values of the resulting η can be compared with those shown on Table 3.1.

5. CONCLUSIONS

From the above discussions it can be concluded that the energy approach is a consistent and reliable method to determine the structural response under earthquake loads. The force based design approach can be used for designing elastic structures but less accurate for highly inelastic structures (large R values). The extent of structural damage is more determined by U_E than by DMF.

AKCNOWLEDGEMENT
The author wishes to thank to all parties that makes this publication possible. Amongst others are researchers who have contributed the experimental data and to the students and fellow faculty members involved in the IMHERE research. The IMHERE research is funded by the Ministry of Education of the Republic of Indonesia.

REFERENCES

Akiyama H (1985). Earthquake Resistant Limit State Design for Buildings. University of Tokyo Press.

Akiyama H (1988). Earthquake resistant design based on the energy concept. *Proc. 9th WCEE, Tokyo*, **5**: 905-910.

American Society of Civil Engineers (2010). Minimum Design Loads for Buildings and Other Structures, ASCE Standard, ASCE/SEI 7-10, Structural Engineering Institute.

Cosenza E, Manfredi G. Seismic design based on low cycle fatigue criteria. *Proc. 11th WCEE*; Acapulco, 1996, Paper No 1141.

Fajfar P, Vidic T, and Fischinger M (1996). On Energy Demand and Supply in SDOF Systems. Nonlinear Seismic Analysis and Design of Reinforced Concrete Buildings, Fajfar P, Krawinkler H (editors), Elsevier, 41-62.

Imran I, Simatupang R, Pamujie E, and Gunawan M (2006). Effects of Steel Reinforcement Types on Plastic Behavior of Special Moment Resisting Frame Element (in Indonesian). *The Annual Indonesian Society of Structural Engineering Conference*, Jakarta.

Institute for Research on Human Settlements/IRHS (2010), Unpublished Test Reports.

Kalkan, E. and Kunath, S.K. (2007). Effective Cyclic Energy as a Measure of Seismic Demand. *Journal of Earthquake Engineering,* **11: 7**25-751.

Kalkan, E. and Kunath, S.K. (2008). Relevance of Absolute and Relative Energy Content in Seismic Evaluation of Structures. *Advances in Structural engineering* **11:1**,1-18.

Mangkoesoebroto SP, Surahman A, Batubara S, and Irawan P (2003). Investigation of full-scale concrete beam column subassemblies. *Proc. Ninth East Asia-Pacific Conference on Structural Engineering and Construction, Bali, Indonesia*, ISBN: 979-3507-047, Paper No 138/RCS-159.

Park YJ, Ang AH, and Wen YK (1985). Seismic damage analysis of reinforced concrete buildings. *Journal of Structural Engineering*, **111**(ST4): 740 – 757.

Surahman, A, (2007). Earthquake-resistant structural design through energy demand and capacity. *Earthquake Engineering and Structural Dynamics*, **36**: 2099-2117.

Surahman, A. (2011). Cumulative Ductility Under Earthquake Loads. *Proceedings, The Second International Conference on Earthquake Engineering and Disaster Management (ICEEDM-II 2011)*, ISBN: 978-602-97462-0-8, Surabaya, July 19 – 20, 31 – 44..

Surahman A and Merati W. (1992). Input energy based seismic design code. *Proc: 10th WCEE; Madrid*, **9**: 5887-5890.

Surahman A, Mangkoesoebroto SP, and Irawan P (2003). Energy absorption capacity of structural components under reversed cyclic loading. Contract No. ITB (INA) 0107 Research Report; AUN/SEED-Net.

Surahman A and Moestopo M. (2000). Analytical and experimental evaluations of earthquake induced stresses on structures for building code purposes. *Contract No 036/HTPP-III/URGE/1997 Research Grant Batch III Report, University Research For Graduate Education,* Directorate General of Higher Education, Ministry of Education and Culture.

Surahman A, Sengara IW, and Merati W (2008). Probabilistic Seismic Hazard Assessment and Structural Performance Against Seismic Actions. *Proceedings, International Conference on Earthquake Engineering and Disaster Management (ICEEDM08)*, ISBN: 978-979-17551-0-8, Jakarta, April 14-15, Paper ID: ICEEDM-007KS.

Teran-Gilmore A, and Jirsa JO. The use of cumulative ductility strength spectra for seismic design against low cycle fatigue. *Proc. 13th WCEE* ; Vancouver, 2004, Paper No 0889.